Unclassified

Crystal Growth of Diode Pumpable Laser Materials

Roger F. Belt, Robert Uhrin, Mark Randles, and John Creamer

Final Report

September, 1990 to November, 1993

Contract N00014-90-C-0233

Airtron Division
Litton Systems Inc.
200 E. Hanover Ave
Morris Plains, NJ 07950-2442

NOTICES

This work was sponsored by the
Office of Naval Research
and managed by
Naval Research and Development
Research, Development, Technology, and Engineering Division
Naval Command, Control and Ocean Surveillance Center
San Diego, CA 92152

REPORT DOCUMENTATION PAGE

Form Approved
OMB No. 0704-0188

1. AGENCY USE ONLY (Leave blank)	2. REPORT DATE	3. REPORT TYPE AND DATES COVERED
	31 Jan, 1994	Final, 1 Sept, 1990- 1 Nov, 1993

4. TITLE AND SUBTITLE
Crystal Growth of Diode Pumpable Laser Materials

5. FUNDING NUMBERS
N00014-90-C-0233

6. AUTHOR(S)
R.Belt, R.Uhrin, M.Randles, J.Creamer

7. PERFORMING ORGANIZATION NAME(S) AND ADDRESS(ES)
Airtron Division
Litton Systems Inc
200 E. Hanover Ave
Morris Plains, NJ 07950

8. PERFORMING ORGANIZATION REPORT NUMBER

9. SPONSORING/MONITORING AGENCY NAME(S) AND ADDRESS(ES)
Office of Naval Research
Naval Research and Development
Research, Development, Technology, and Engineering Division
Naval Command, Control and Ocean Surveillance Center
San Diego, CA 92152

10. SPONSORING/MONITORING AGENCY REPORT NUMBER

11. SUPPLEMENTARY NOTES
None

12a. DISTRIBUTION/AVAILABILITY STATEMENT
Distribution not limited

12b. DISTRIBUTION CODE

13. ABSTRACT *(Maximum 200 words)*

This program describes the preparation and crystal growth of materials which may be particularly suitable for laser diode pumping. Disordered crystal structures with broadened absorption and emission bands were investigated. About 60 growth runs were achieved with oxide hosts and ten with fluoride hosts. The laser dopants were chosen to yield highly efficient 1-5 μm lasers, possible tunable laser in the 2-3 μm region, all with good temperature stability. Materials were all grown, fabricated, and coated at Airtron. The active and passive laser tests were performed at the Naval Research Laboratory. Several oxides were identified and gave excellent results with Ho, Er, or Tm doping. U^{3+}:$YLiF_4$ was the most interesting among the fluorides. The results of these investigations were presented at various conferences.

14. SUBJECT TERMS	15. NUMBER OF PAGES
Crystal growth, Czochralski method, laser materials, single crystals, mixed oxides, fluorides	64
	16. PRICE CODE

17. SECURITY CLASSIFICATION OF REPORT	18. SECURITY CLASSIFICATION OF THIS PAGE	19. SECURITY CLASSIFICATION OF ABSTRACT	20. LIMITATION OF ABSTRACT
Unclassified	Unclassified	Unclassified	None

Table of Contents

List of Figures

List of Tables

1.0 Introduction

Rapid strides have been made in the laboratory preparation of laser emitting diodes[1]. Over the past few years, power outputs have continued to rise to more than 1W and diodes have become feasible as pump sources for Nd^{3+} doped laser materials[2]. Most of these recent experiments were performed with single diodes in a longitudinal (end) pumped configuration using commercial Nd^{3+} doped laser hosts such as glass, YAG, YLF, YALO, BEL, garnets and YVO_4. However laser diode arrays are under intensive development[3] and offer outputs up to 50W. With these multiple diode arrays, transverse pumping becomes very efficient. High energy per pulse and high average power are attainable[4]. In fact, as the cost of the arrays continues to decrease and power output increases to 1 $J/cm^2/ms$, diode arrays may even pump amplifiers for many high power applications[5].

Diode pumping of lasers is attractive because of potential low cost, high efficiency, compact geometry, robust construction, and long life. A most important goal for rare earth doped materials is to maximize the output efficiency. For transverse diode pumping, efficiency is quite dependent on the choice of the laser material. The efficiency of any material can be estimated from its absorption spectra, upper laser level lifetime, and stimulated emission cross section. Overall laser device efficiency depends directly on the material and is a function of absorption, quantum, storage, and extraction efficiencies. For six prominent commercial laser hosts, a thorough analysis has been performed [6] and conclusions reached for several modes of operation.

A deliberate search for new efficient Nd^{3+} doped laser hosts should rely on several known and measurable parameters. Among these are high peak absorption, a broad absorption band, a long upper level lifetime, a high emission cross section, and a high gain coefficient. Not all of these are independent and may depend on other parameters such as inversion density, length of material, and concentration of Nd^{3+}. For pulsed operation Nd:YAG and Nd:$YLiF_4$ are two of the best present materials. However a CW or high average power laser may have different design criteria and different conclusions may be reached. For many applications the final design is not known but we investigated materials which are likely to yield improvements because of the host properties.

The principal objective in our investigation was the identification of potential new laser hosts which will lead to highly efficient diode pumped lasers. The main criteria in our search was peak absorption, absorption line width, emission cross section, gain coefficient and upper level fluorescent lifetime. Obviously these were parameters to be measured and compared after choices are made and various materials are grown. Unfortunately there were few theoretical principles which lead unambiguously to the right materials. The situation was not helpless though since large deposits of empirical data have been collected at least for Nd doped materials[7]. These data gave important clues for discovering new hosts with desirable crystal structures which generally yield a favorable property.

The trivalent ion Nd^{3+} has been inserted in more than 300 different host crystals and the energy levels are very well characterized. The Nd^{3+} always has

its absorption bands centered near 540, 580, 760, 800, and 870 nm. The principal laser transitions for this four level system are centered about 1064, 1120, 1340, and 940 nm. The 800 nm absorption and 1064 nm emission are the most efficient combination. The broadest absorption for Nd^{3+} occurs in low gain, completely disordered materials such as glass. Narrowest line absorption conversely occurs in ordered crystals as YAG. Our problem was to search for partially disordered hosts which have intermediate linewidths, gain coefficients, and high lifetimes. Notice that in general, fluoride hosts have higher lifetimes than oxides. For disordered fluorides the lifetime is the highest. Some other empirical "rules" were also informative[8]. Thus it was found that: (1) concentration quenching of lifetimes is found in centrosymmetric structures with isolated polyhedra (2) longer lifetimes are found in centrosymmetric structures usually accompanied by larger cross sections (3) symmetry of local sites, particularly the anion configuration, does influence lifetime[9]. Because of its large physical size the Nd^{3+} can only be incorporated easily into host structures which contain sufficient space for it. Thus a lot of structures are eliminated among the low atomic number elements.

Laser action beyond 1064 nm has been associated with Er^{3+}, Tm^{3+}, Ho^{3+}, Dy^{3+}, and U^{3+}. Single and multiple doping with energy transfer schemes have led to some fairly efficient lasers. However this area has not been investigated as thoroughly as the Nd^{3+} doped materials. The principal problems were manifold. First we mention that pump sources such as flash lamps or tunable lasers had to be used. Laser diodes emitting near 800 nm were satisfactory for

only a few special situations such as Er or Tm[10-13]. Secondly the multiply doped systems were most efficient at very specific concentrations of several ions. This greatly increased the materials preparation and optimization schedules for each lasing system. Thirdly, recent military programs have just begun to fund laser development for selected applications in 1.5-5 μm. Fortunately, some medical applications have also spurred research.

The principles elicited for Nd^{3+} above apply directly to other smaller sized rare earth ions which can lase over 1.5-5 μm. Thus the same hosts suggested for Nd^{3+} can be adapted to Er, Tm, Ho, and Dy. The special case of U^{3+} has to be treated differently. It is not likely to be incorporated in the high melting oxides but must be introduced in low melting fluorides to avoid U^{4+} or U^{6+}.

A major problem after host selection was optimizing the amount of each dopant. This was host dependent. In our initial survey those ions and concentrations which worked well in YAG or $YLiF_4$ were chosen for the new hosts. Further optimization may be required. A complete solution to efficient infrared lasing may require new diode pump wavelengths, favored energy transfer schemes, and a comprehensive examination of the best new hosts.

2.0 Experimental Procedures

All crystal growth activities consisted of a parallel effort on the preparation of both oxide and fluoride laser hosts. A general plan was followed whereby a desired list of potential crystals was compiled first. This list was arrived at by detailed quarterly discussions between the Airtron crystal growers and laser physicists at the Naval Research Laboratory. From each completed material list,

Airtron proceeded to grow crystals with the requisite dopants and specified concentration levels. The order of growth was chosen in a manner whereby the easiest crystals were completed first and the more difficult hosts were deferred until later. This strategy was chosen for the following reasons: (1) the growth cycle for a crystal may approach a few weeks (2) fabrication and coating for a particular material may consume a few more weeks (3) once our process was started, we always had a deliverable stream of crystals ready for further passive or active testing (4) the chosen method represented the most efficient utilization of contract funds. If a particular host crystal was too difficult to grow after a few attempts, that crystal was abandoned. This approach prevented our program from being entangled in lengthy material growth problems.

2.1 Growth of Oxides

The starting components for mixed oxide growth were purchased as 99.99% or better purity. Sometimes a component was added in the form of a carbonate. The yttrium and rare earth oxides were analyzed with respect to those elements only. However the residual non rare earths were normally less than 100-150 ppm and consisted of Ca, Mg, Si, Al or other elements of low atomic number. Components were purchased from qualified vendors such as Shinetsu of Cleveland, Ohio, Showa Denko of New York, Aran Isles of Rockport, MA, UMC of Lindhurst, NJ, Eagle Picher of Quapaw, OK, Johnson Matthey of Philadelphia, PA, Bicron Corp. of Newberry, OH, and Alpha of Ward Hill, MA.

All oxides were grown from melts contained in iridium crucibles. The crucible dimensions were 2 or 3 inch diameter, 2 or 3 inch height, and 0.080 to

0.100 inch wall thickness. The vendor was Engelhard Minerals and Chemicals of Carteret, NJ. After a growth run was performed, the crucible was cleaned of its residual contents by chemical flux dissolution or acid treatments. If a new composition was prepared which was similar to the previous one, the melt was reformulated and used again where possible.

Seed crystals were frequently a problem particularly in those crystals which were never grown at Airtron previously. Under these circumstances seeds were obtained by initiating growth on a wire or obtaining a segment from the cooled melt. For crystals such as garnets, perovskites, silicates, or other common hosts, Airtron had an extensive supply of seeds which were available readily.

The seed crystal orientation was always controlled and usually performed by Laue X-ray back reflection methods. For the cubic garnet hosts, the normal orientation was [111] as the boule axis. In other non cubic hosts, a major direction was chosen along a or c for uniaxial materials. Some crystals may have a preferred growth direction located off a main direction. This effect is due to the details of the crystal structure and some of the unique physical properties such as thermal conductivity or expansion. These artifacts are revealed during growth and in such cases it is best to allow the crystal to grow as it desires.

All oxides were grown in a basic Czochralski station as typified by Fig. 1. This illustration does not show the power supply for the RF coil, the pulling and rotation mechanisms, and the diameter control system. The latter may be of two different types. One early system utilized an optical pyrometer which focused on

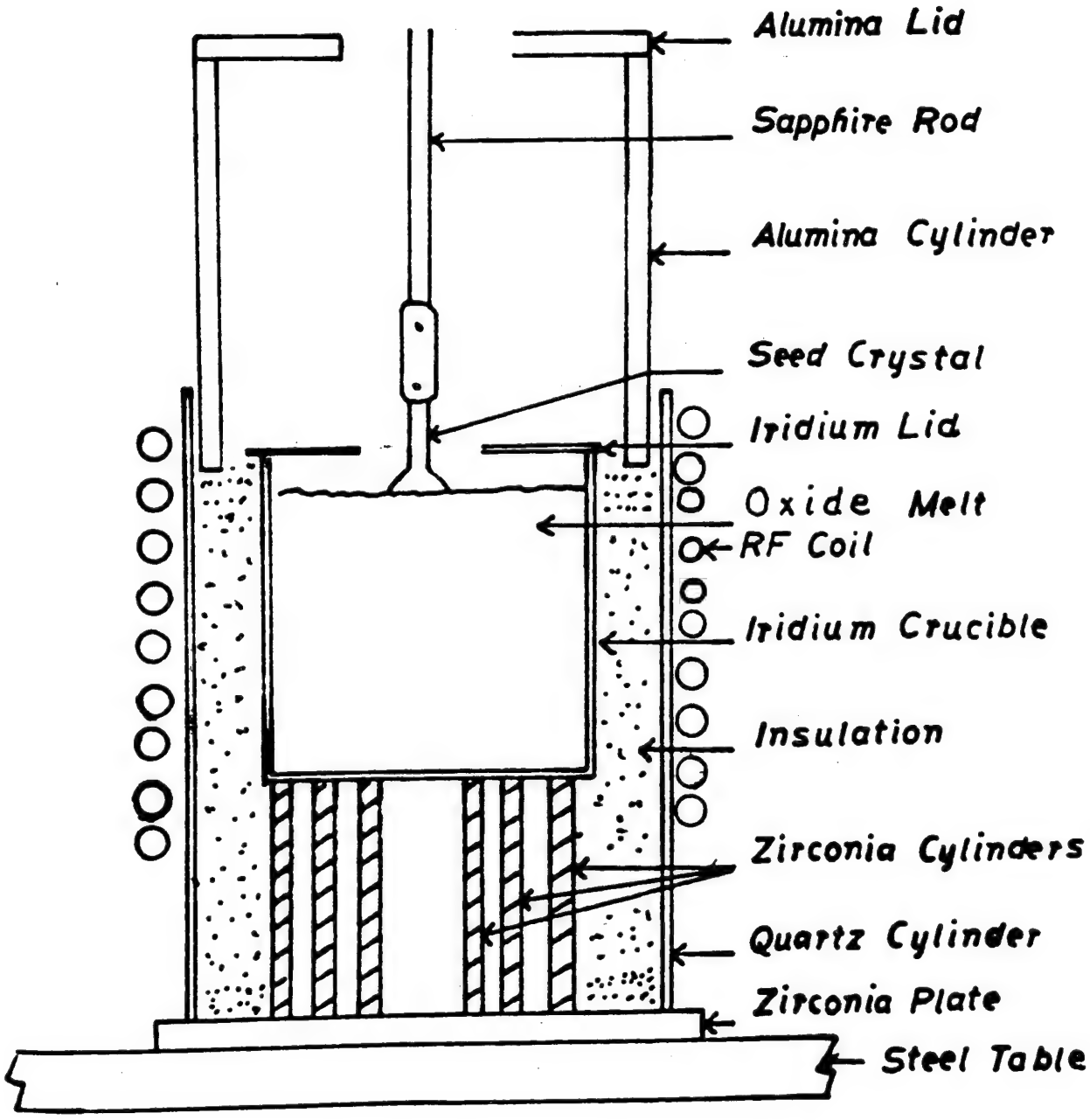

Fig. 1 Line Drawing of Czochralski Growth Station

the meniscus surrounding the growing crystal. Later crystals were grown at Charlotte, NC where a computer controlled crystal weighing system was employed. For the crystals grown, each system worked well and held the diameter to within a variation of only a few per cent over periods of three weeks. Fig. 2 is a photograph of a complete station used in our program.

The process for growing a crystal was developed over years of experience. The chemical components are first weighed and then mixed thoroughly. The growth station is then prepared with particular attention given to the placement of the iridium crucible within the geometry of Fig. 1. The crucible is filled with as much powder as possible and then placed within the station. A seed crystal is chosen and attached to the pulling shaft. The enclosure for the system is put in place and the gas mixture of N_2-0_2 is started flowing at the desired rate. The crucible is heated by RF currents until all powder melts. At this stage the remaining charge is added to bring the melt level to the desired position. The seed crystal is then dipped and temperature is lowered to increase the crystal diameter. The automatic controls are adjusted to bring the crystal to desired diameter and length. At the attainment of proper length, the crystal is pulled free of the melt and annealed in place by a gradual lowering of temperature. The cooled crystal is removed from the seed and is readied for future processing steps.

2.2 Growth of Fluorides

Fluorides present a special problem in crystal growth because most rare earths and many other components are not available commercially in high purity.

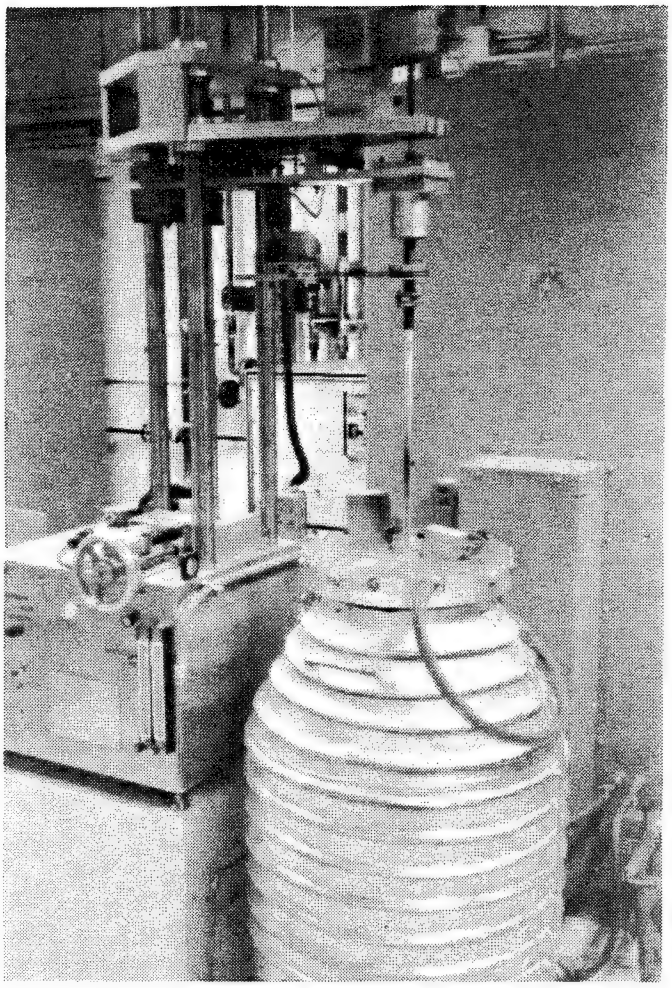

Fig. 2 Photograph of Operating Growth Station

Therefore our strategy has been to purchase the high purity oxides and convert them to the fluorides via a hydrofluorination reaction as given in equation 1 below.

$$R_2O_3 + 6HF \longrightarrow 2RF_3 + 3H_2O \qquad (1)$$

In this equation, R may be any rare earth La → Lu or Y. Reaction 1 is not performed in solution but under anhydrous gas-solid conditions where conversion is complete. Under these circumstances the fluoride contains only traces of any O^{2-}, OF^-, or OH^-.

Seed crystals of $YLiF_4$, BaY_2F_8, $LiCaAlF_6$ and others were available from previous programs and did not require special growth runs. The $YLiF_4$ and $NaYF_4$ structures are uniaxial and crystals were generally grown along an a axis. BaY_2F_8 and its isomorphs are biaxial monoclinic structures. However the crystal prefers to grow off a major axis. In this circumstance crystals were grown along that natural unknown direction. Detailed studies have been made subsequently of the effects of laser gain on crystal orientation.

Our investigations were also concerned with the introduction of U^{3+} into laser hosts such as $YLiF_4$. Since UF_3 could not be purchased, we prepared this material from a mixture of powdered Al and UF_4 via the reaction 2

$$3UF_4 + Al \longrightarrow 3UF_3 + AlF_3 \qquad (2)$$

The reaction was carried out at 875-900^{0}C. The AlF_3 is volatile and sublimes out of the hot reaction zone particularly with an inert carrier gas. In order to perform the above reaction, the required stoichiometric amounts of powered UF_4 and powdered aluminum were mixed dry. The mixture was placed in a graphite boat

and heated gradually to 900°C while passing argon gas over the mixture. Heating above 900°C was avoided since some disproportionation can occur via the following reaction

$$4UF_3 \longrightarrow 3UF_4 + U \qquad (3)$$

The U^{3+} is a weak α emitter and safety precautions were taken. The UF_3 was checked by X-ray diffraction to be of single phase.

A drawing of our hydrofluorination reactor is given in Fig. 3. The body tube construction was entirely from platinum. This enabled us to carry out the reaction of any oxide at temperatures up to 1250°C. For most rare earth oxides the preliminary reaction was performed at 800-850°C. After reaction was completed, the temperature was raised to 1200°C. This was sufficient to melt the polycrystalline fluoride and large single crystal pieces were usually obtained. All materials were placed in a platinum boat which rested on a carbon block. Our platinum tube was heated resistively with a high current and low voltage power supply. A photograph of the completed apparatus is given in Fig. 4. Insulation covers the platinum tube. The power supply is located under the table. This apparatus has given good service and has run for years without a HF leak. In practice, a composition can be formulated for all the host and dopant components which are then converted to fluorides. In the growth cycle, only additional LiF, BaF_2, or other fluoride has to be added to the material.

The growth station for fluorides was a design which could utilize HF as a growth atmosphere at temperatures up to 1000°C. With an inert gas the high temperature limit was about 2000°C. In order to reach these temperatures, a

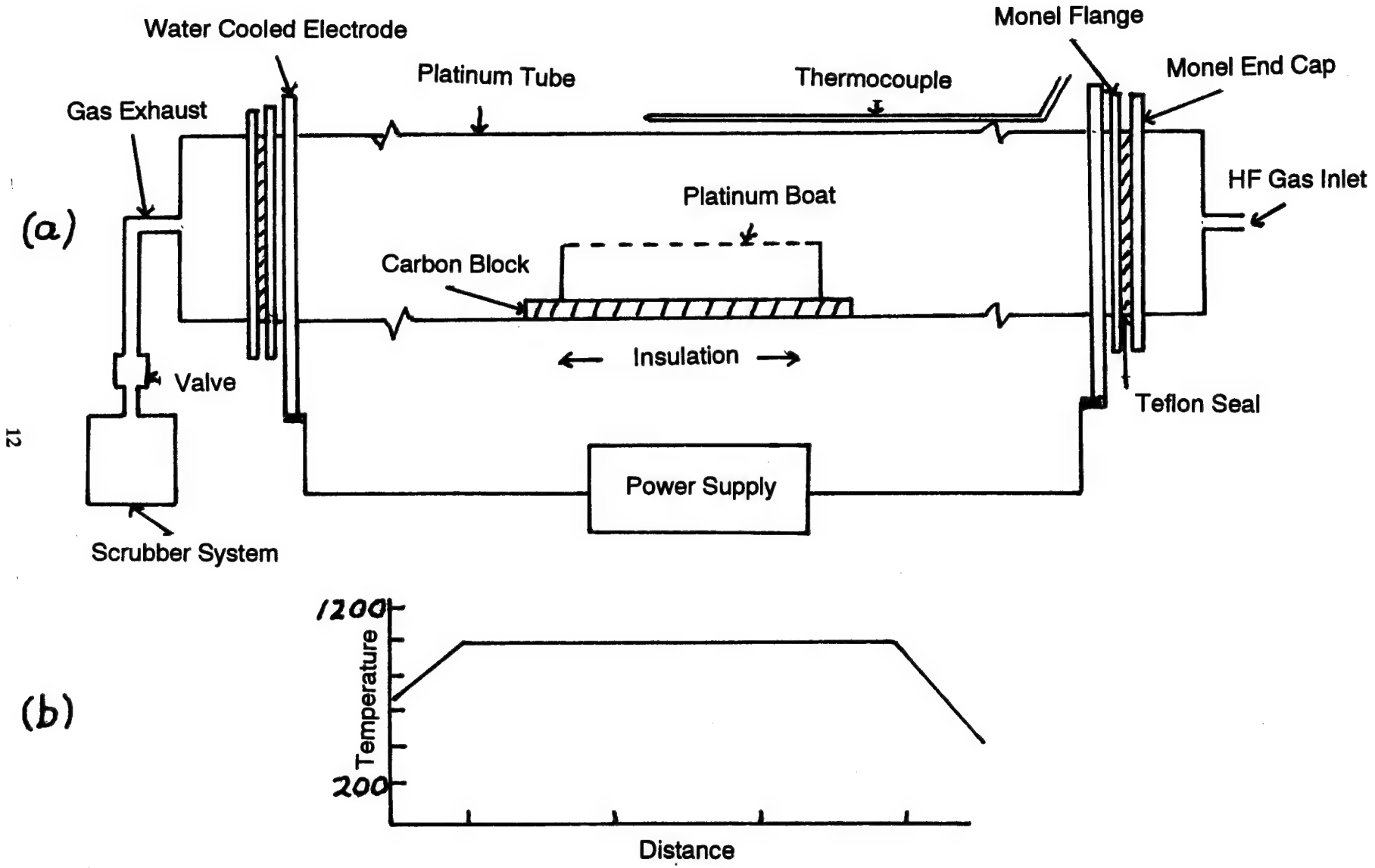

Fig. 3 (a) Line Drawing of Hydrofluorination Reactor
(b) Profile of Furnace Temperature

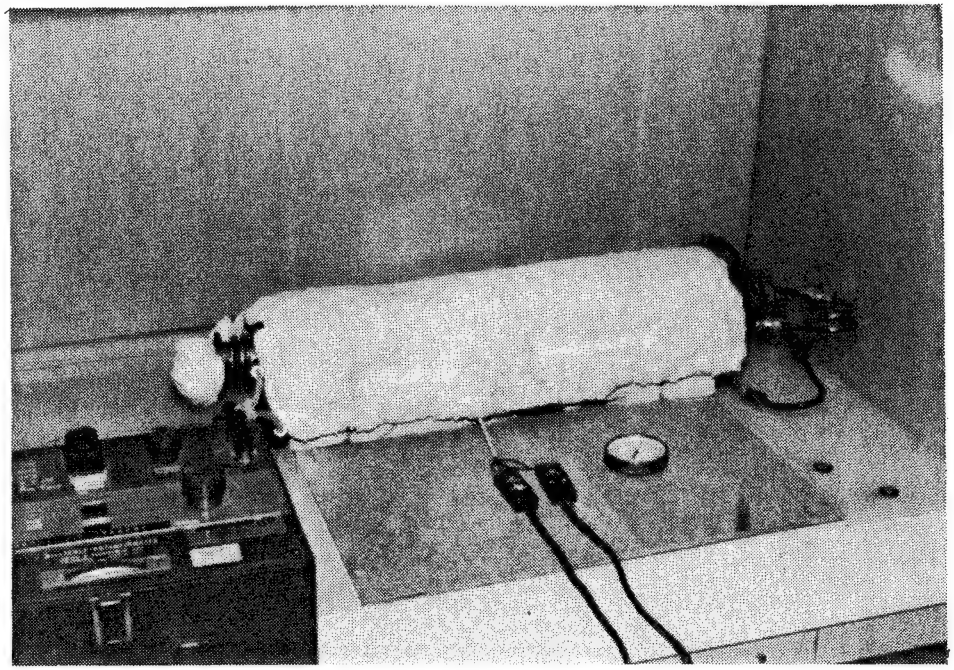

Fig. 4 Photograph of Hydrofluorination Apparatus

resistively heated graphite element was employed. The growth chamber was water cooled and plated with nickel inside to minimize corrosion. All interior insulation was prepared from non oxidic materials. The crucible for melt containment was generally platinum or glassy carbon. The method of diameter control was achieved by direct weighing of the crystal via a load cell. Either an analog system or computer was used to program the crystal shape to the desired diameter and length. Basically, the Czochralski method was used even though for many crystals a solution was employed rather than a pure melt. A photograph of one of our stations is given in Fig. 5. The power supply is located at the left of the growth chamber.

2.3 Material Fabrication

After a crystal was grown, a number of processing steps were performed in order to attain a specific size, shape, orientation, and coating for the intended application. Samples such as disks, rectangular parallelepipeds, cylindrical rods, and curved end face rods were typical. Most of these were chosen as a function of the particular pump source available; single laser diodes, diode arrays, and other lasers were typical of the pump sources. The geometry of the laser test was also important. At times end pumping was useful, sometimes side pumping, and even flashlamps were employed if lasers were not available.

The rough crystal is mounted on a holder and X-ray oriented to confirm the boule growth direction and optical axes. For rectangular samples, a rough sample is cut by means of a saw (Fig. 6) and 90^0 rotation of the boule. For rods, the boule is mounted on one flat end and core drilled with a diamond drill. At

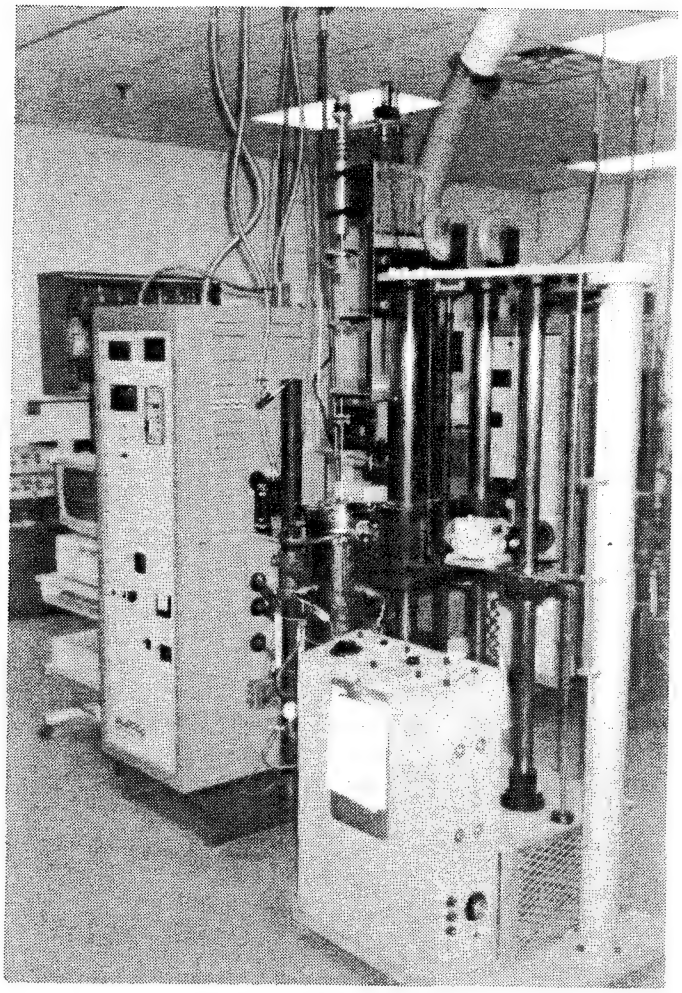

Fig. 5 Photograph of Fluoride Growth Station

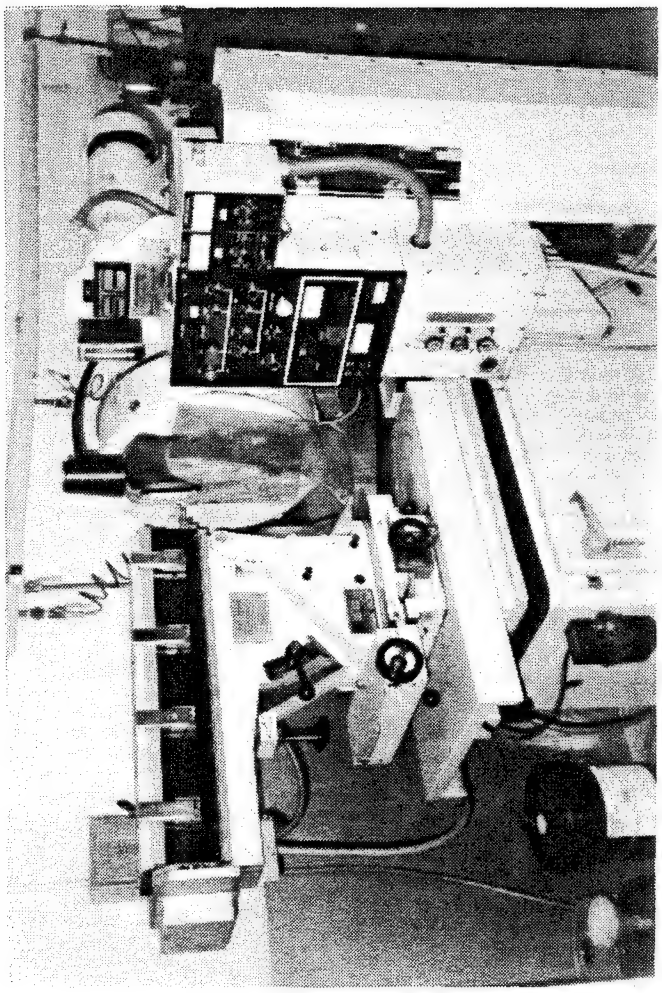

Fig. 6 Crystal Cutting Equipment

this stage, the rough samples are mounted in special polishing fixtures where one, two, or three pairs of opposing faces are finished flat, parallel, and to the desired laser specifications (Fig. 7). The dimensions, angles, face flatness or curvature, perpendicularity, or other requirements are checked constantly by in-process measurements. Ordinary and special tools are used for these tests. After attaining the desired specifications, each laser piece is removed from its fixture and prepared for any optical coatings.

The optical coatings for each submitted sample were of special design and determined by the intended active tests. Some coatings were a simple single band anti-reflection (AR) type formulated for the lasing wavelength. The latter was normally close to the 1.06, 2.01, 2.93 μm or other lasing wavelength. Other coatings were so called dual band; i.e. highly transmitting at the diode laser pumping wavelength and highly reflecting at the actual materials lasing wavelength. The design of each coating was performed with the assistance of refractive indices, polarization, desired transmitting or reflecting characteristics, and a computer software program[14] written for the purpose. The actual films were deposited by means of resistive, electron-beam, or other heating of fluorides or oxides. Commercial or Airtron designed vacuum stations (Fig. 8) with optical thickness monitors were used. The films were single layer or more complicated multi-layer configurations with high and low index components.

2.4 Testing of Materials

Materials testing consisted of both passive and active measurements on each delivered sample. For convenience, all of the passive tests associated

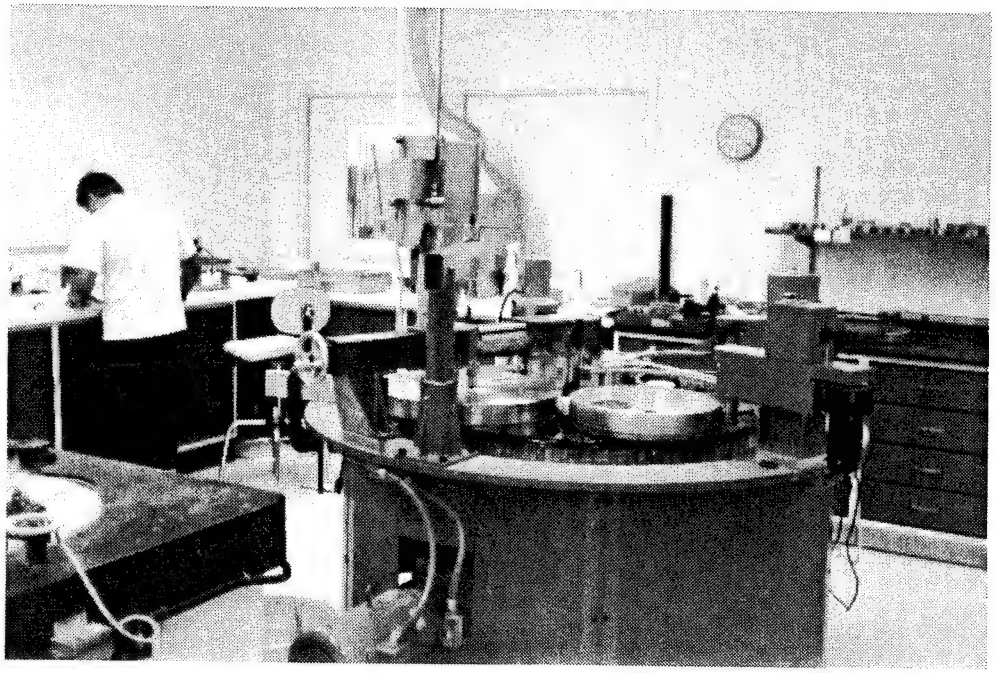

Fig. 7 Crystal Polishing

Fig. 8 Optical Coating

with sample fabrication were performed at Airtron. These included the crystal orientation, geometry and dimensions, dopant concentrations, specifications on flatness, parallelism, and perpendicularity, transmission or reflection characteristics of the optical coatings, and any other necessary tests.

The bulk of the laser associated testing was performed at the Naval Research Laboratory, Washington, DC. These tests included the absorption spectra, fluorescent lifetime of excited states, the emission spectra of fluorescence under varied excitation, and further lasing parameters as measured under active testing. A summary of any detailed work was generally presented at a major conference on lasers.

3.0 Results of Crystal Growth

Crystal growth of both oxide and fluoride host crystals was investigated under our program. These hosts were chosen mainly to obtain absorption bands which were broadened somewhat and easily overlapped the diode emission. In this manner, efficiency of pumping should remain high and temperature effects are minimized. We first look at the host crystal and its effect on various laser properties.

3.1 Host Effects on Laser Parameters

Wavelength of Emission

The lasing wavelength of a diode pumped solid state laser depends foremost on the paramagnetic ion and the energy levels of the laser transition. For the 1-5 micron wavelength range the ions with demonstrated performance as room temperature lasers are primarily the rare earths as listed in Table I.

Table I

Efficient Laser Transitions at 1-5 microns
in Oxides & Fluorides at Room Temperature

Ion	Upper Laser Level	Lower Laser Level	Wavelength (μm)
Nd^{3+}	$^4F_{3/2}$	$^4I_{11/2}$	1.06
Nd^{3+}	$^4F_{3/2}$	$^4I_{12/2}$	1.35
Ho^{3+}	$^5I_7$	$^5I_8$	2.05
Ho^{3+}	$^5I_6$	$^5I_7$	2.9
Ho^{3+}	$^5I_5$	$^5I_6$ (cascade $LiYF_4$)	3.9
Er^{3+}	$^4I_{13/2}$	$^4I_{15/2}$	1.6
Er^{3+}	$^4S_{3/2}$	$^4I_{9/2}$	1.7
Er^{3+}	$^4I_{11/2}$	$^4I_{13/2}$	2.8-2.9
Tm^{3+}	$^3H_4$	$^3H_6$	1.95
Tm^{3+}	$^3F_4$	$^4H_5$	2.35
Dy^{3+}	$^6H_{13/2}$	$^6H_{15/2}$	3.0
U^{3+}	$^4I_{11/2}$	$^4I_{9/2}$	2.6

Neodymium is the most efficient at 1 micron and holmium, erbium, dysprosium, and thulium are typically used to generate 1.5-5 microns. U^{3+} has been lased at 2.6 microns in CaF_2, and the Ho 3.9 μm line has been demonstrated by cascade operation of Ho:$YLiF_4$ with a 532 nm pump[15]. Other cascade schemes are possible. Laser wavelengths achieved are tabulated in several volumes[7, 16].

The host crystal perturbs the active ion by the symmetry and strength of the crystal field at the ion site. For the rare earth ions with shielded 4f electrons the crystal field causes splitting of the energy levels, called the Stark effect. The modified energy levels produce laser transitions that vary slightly in wavelength. The fluorescence is not a single wavelength, but a set of closely space lines. These lines can be discrete or overlapping, which permits laser operation to be tunable over a limited range. For example, a Tm:YAG laser has been tuned over the range of 1.87 to 2.16 microns[17].

Transitions in fluoride hosts can be shifted up or down from those of the oxides because of modifications to the crystal field from a greater variety of crystal structures, site symmetries, and differences in binding energy between oxygen and fluorine ions.

Linewidths of Emission and Absorption

The typical laser diode has an emission linewidth of 2-3 nm and the wavelength varies with temperature. The temperature may change with ambient operating conditions. An array of diodes could have a larger wavelength spread. A high quality crystal such as YAG has an absorption line of about the same width. For example. the absorption peak in Tm:YAG at 795 nm is only 3 nm

wide[18]. It becomes a technological problem to keep the laser diode pump in the absorption band. An improved host should have an absorption linewidth on the order of 5-10 nm.

One relative comparison of the linewidth variations for different hosts is the fluorescence peak width. Table II shows the range of linewidths of the Nd $^4F_{3/2} \longrightarrow {}^4I_{11/2}$ transition in several crystals at room temperature [16]. The table illustrates the linewidth variations made possible by tailoring the composition of the host crystal. Airtron has investigated new hosts and examined some known hosts with regard to optimization of diode pump absorption linewidth, while maintaining other desirable characteristics, such as lifetime and gain. A host that has the proper rare earth site for Nd is likely to also provide a good site for the other rare earth ions, such as Ho, Er, or Tm.

Lifetime and Gain

The fluorescence lifetime of the upper laser level depends on the host crystal through phonon interactions and other nonradiative processes. In a typical 4-level laser, phonons depopulate the lower laser level and assist in the population of the upper laser level by relaxation from higher energy excited states. A large population inversion is essential for efficient laser operation. Low threshold operation is achieved when the nonradiative decay rate of the upper level is small compared to the radiative rate, resulting in a long fluorescence lifetime.

One source of nonradiative decay is concentration quenching, a host related effect which depends on the separation between rare earth sites in the

Table II

Fluorescence Linewidth of the Nd $^4F_{3/2} \longrightarrow {}^4I_{11/2}$ Transition in Various Crystals at Room Temperature

Host	Degree of Disorder	Linewidth (nm)
YAG	low	0.7
YVO_4	slight	0.9
YSGG	slight	0.9
$LiYF_4$	moderate	1.4
Y_2SiO_4	moderate	1.4
$CaY_4(SiO_4)_3O$	high	5.9
$LiLa(MoO_4)_{12}$	high	11
$Na_5Y_9F_{32}$	high	11
CaF_2-SrF_2-BaF_2	mixed crystal	11

crystal. Energy exchange between nearest neighbors causes depopulation of the upper laser level. Many crystals may only be doped to 1 or 2% Nd before the fluorescence lifetime decrease becomes intolerable, but a high Nd concentration is desirable to reduce the optical absorption length for the pump radiation. Not all rare earths are similarly affected by concentration quenching due to differences in their energy level structure. Ho and Er in particular can be heavily doped with minimal degradation.

Nonradiative decay is also caused by crystalline defects, such as color centers, quenching impurities, vacancies, etc. To fully evaluate a host with specific dopant additions the crystal should be of excellent quality. The Czochralski technique for the growth of oxides and fluorides produces crystals of high quality.

Site Order and Absorption

It was desirable to develop a laser and activator host combination with a wider absorption band. The linewidth in crystals may be either homogeneously or inhomogeneously broadened. The homogeneous broadening is caused by phonon coupling to the lattice which alters the crystal field. All ions participate equally and stimulated emission can occur for photons anywhere within the linewidth, resulting in high gain. Homogeneous broadening is typical for 4f transitions of the rare earths in highly ordered, high quality crystals such as YAG, which has only rare earth site.

Inhomogeneous line broadening is caused by site-to-site disorder in the crystal field. Such random variations may be caused by strain, defects, impurity

ions or compositional variations. Some hosts have nonequivalent rare earth substitution sites. For example. lanthanum magnesium aluminate (LMA) $LaMgAl_{11}O_{19}$ has three sites with slightly different crystal fields. As a result neodymium doped LMA shows fluorescence linewidths that are an order of magnitude larger than Nd:YAG. The pump bands are similarly broadened. Nd:LMA has been operated as a CW laser with selectable operation at 1.054 and 1.082 microns and each band has several nm of tuning range. LMA is a good crystal to investigate with other rare earth substitutions.

Line broadening also occurs in some fluorides as a result of two-site occupancy (e.g. $NaYF_4$). Additionally, this property is also affected by interstitial fluorine ions resulting from charge compensation for trivalent rare earth ions on alkali, alkaline earth, and transition metal sites.

3.2 Oxide Hosts for Nd

The Czochralski method was applied to the growth of selected oxides with the goal of developing improved crystals for diode laser pumped lasers. The selection criteria below were used to screen the candidate materials. The materials selected were not well characterized or they had crystal growth problems.

Selection Criteria for Oxide Laser Host Crystals:

1. Substitution sites for Nd, Ho, Er, Tm, or other rare earths
2. Moderate to high site disorder expected
3. Good mechanical properties

4. Congruent melting composition

5. Optically transparent at the wavelength of interest

Based on the above criteria, Airtron prepared a list of Nd-doped disordered oxide crystals to investigate as in Table III. Nd:YVO_4 can be a highly efficient diode pumped laser, but a persistent problem with yttrium vanadate was the formation of color centers during Czochralski growth. This was likely the result of a reduction of the valence of some of the vanadium ions from the desired V^{+5} to V^{+4} or loss of V_2O_5. High temperature annealing in an oxidizing atmosphere helped decrease the number of color centers. As an alternative we investigated a melt compensation scheme that eliminated the need for post-growth annealing.

The four hosts $Ca_3Ga_2Ge_4O_{14}$, $Sr_3Ga_2Ge_4O_{14}$, $La_3Ga_5Ge_1O_{14}$, and $La_3Ga_5Si_1O_{14}$, have been reported in the Soviet literature and they appear to have a moderate degree of site disorder. The large Ca, Sr, and La sites allowed for easy Nd substitution.

$SrGdGa_3O_7$ and $CaYAl_3O_7$ are only two members of the class of crystals called melilites, which have an inherently disordered structure. Many congruent compositions exist with the general formula ABC_3O_7 where A=Ca, Sr, Ba; B=La..Gd; and C=Al, Ga. Several of these materials have recently been grown as small fibers[21] and they appear promising. With 1% Nd doping: $CaYAl_3O_7$ has a lifetime of 175 microseconds and an absorption linewidth of 4.6 nm; $SrGdGa_3O_7$ has a lifetime of 202 microseconds and a linewidth of 8 nm. Note that Nd can replace either the divalent ion (Ca, Sr) or the trivalent rare earth (Y, Gd). This probably accounts for the increased line widths. In principle the Nd

Table III

Some Disordered Oxide Crystal Hosts

Host	Crystal Structure	Comments
YVO_4	Tetragonal	Slight disorder color centers
$Ca_3Ga_2Ge_4O_{14}$	Trigonal	Disordered
$Sr_3Ga_2Ge_4O_{14}$	Trigonal	Disordered
$La_3Ga_5Ge_1O_{14}$	Trigonal	Disordered
$SrGdGa_3O_7$	Tetragonal	Two site occupancy
$CaYAl_3O_7$	Tetragonal	Two site occupancy

substitution for Ca or Sr can be varied by the number of charge compensating ions in the melt. This provides an interesting method to tailor the width of the absorption and fluorescence lines.

3.3 Description of Grown Oxides

A list of all our growth attempts on particular oxides is given in Table IV. This list provides a chronological order of each attempt, the run station designation, the host composition, dopant and its concentration, and other growth conditions. At certain times, no complete crystal was obtained because the run was a preliminary seeding operation. However for most attempts, a crystal was grown and enough material was obtained for laser characterization.

As mentioned in earlier sections, our general objectives were to examine laser hosts which may be suitable for operation beyond the 1.06 μm of Nd. In a few cases however, some crystals were grown with Nd doping. Particular hosts were chosen with a high amount of disorder. We summarize the class of Nd doped materials in Table V. The amount of Nd is listed together with some comments on the active laser test results.

In order to examine candidates for 2-3 μm lasing, more attention was given to dopants of Tm^{3+}, Er^{3+}, and Yb^{3+}. These were doped singly or in combination with Cr^{4+} which could lead to a fairly efficient energy transfer scheme. The data for Tm^{3+} doped crystals are listed in Table VI. In any work of our type, there are always a few surprises. One of the most promising new materials was CaYSOAP doped with 6% Tm, which for E//c shows an unusually high absorption coefficient: $34cm^{-1}$ at 790 nm and a peak width of 5 nm. The

Table IV.

List of Grown Oxides

Serial #	Run #	Host	Dopant at %	Comments	Growth Axis	Pull Rate mm/h	Rot. Rate RPM	% O_2	Final Boule Disposition
1	B32-363	$CaYAl_3O_7$	---	incongruent, no boule	---	---	---	---	no boule
2	B32-372	$SrGdGa_3O_7$	---	nucleated on Ir wire	---	6	5	2	no boule
3	B32-373	$SrGdGa_3O_7$	---	seed boule	(110)	3	5	2	
4	B32-375	$SrGdGa_3O_7$	6% Tm	blue flourescence, heavy scatter	(100)	1.5	5	2	
5	B32-376	$SrGdGa_3O_7$	12% Tm	blue fluor., very heavy scatter	(001)	1.5	5	2	
6	B32-377	$SrGdGa_3O_7$	3% Tm	blue fluor., bubble core	(100)	1	5	1.5	
7	B32-378	$SrGdGa_3O_7$	2% Nd	bubble core	(100)	1	5	1.5	
8	B32-382	$La_3Ga_5SiO_{14}$	---	seed boule, cracks	10°off (001)	6	5	2	
9	B32-383	$La_3Ga_5SiO_{14}$	---	seed boule, grains & cracks	(001)	1.5	5	2	
10	B32-384	$La_3Ga_5SiO_{14}$	2% Nd	brown, bluer w/N_2 anneal, 2 large facets on interface	a-axis, (11.0)	1.5	5	2	
11	B32-385	$La_3Ga_5SiO_{14}$	4% Nd	grown in N_2, blue, deeper interface	a-axis, (11.0)	1.5	5	0	
12	A13-136	$SrGdGa_3O_7$	4% Nd	bubble core and veils	(100)	1	5	1.8	

Table IV

List of Grown Oxides

Serial #	Run #	Host	Dopant at %	Comments	Growth Axis	Pull Rate mm/h	Rot. Rate RPM	% O_2	
13	A12-210	Y_2SiO_5	---	seed growth on wire, transparent single crystal		6	10	0.3	
14	A12-214	$La_3Ga_5GeO_{14}$	---	seed boule, yellow, density 5.92g/cc	a-axis, (11.0) LGS seed	3	5	2.3	
15	A12-215	$La_3Ga_5GeO_{14}$	2% Nd	reload to undoped run, blue single crystal start but soon became poly	a-axis, (11.0) LGS seed	1.5	5	1.0 (cool 0.2%)	
16	A12-216	$La_3Ga_5GeO_{14}$	2% Nd	fresh melt, blue single crystal start but soon became poly	a-axis, (11.0) LGS seed	1.5	5	1.0 (cool 0.2%)	
17	A12-217	$La_3Ga_5GeO_{14}$	2% Nd	fresh melt, blue single crystal start but became poly after 3cm	c-axis, (00.1) LGS seed	3	5	2.3 (cool 0.2%)	
18	A12-218	$SrGdGa_3O_7$	30% Er	no crystal, two phase liquid?					no boule
19	A12-219	$SrGdGa_3O_7$	5% Er	polycrystalline material				tried 0.35-3%	no boule

Table IV

List of Grown Oxides

Serial #	Run #	Host	Dopant at %	Comments	Growth Axis	Pull Rate mm/h	Rot. Rate RPM	% O_2	
20	A12-220	$CaLa_4(SiO_4)_3O$	0.1% Cr 6% Tm	high scatter,green core, cracked on saw	near (00.1)	3	5	1.6	
21	A12-221	$CaLa_4(SiO_4)_3O$	0.1% Cr 6% Tm	no scatter, uniform blue-green, cracked	near (00.1)	1	5	1.0	
22	B32-409	YVO_4	1.6% Nd	some scatter, cracked	(001)	1	5	0.8	
23	B32-410	YVO_4	1.2% Nd	some scatter, cracked	(001)	1.5	5	0.8	
24	B36-309	$SrErGa_3O_7$	100% Er for Gd	crystal would not grow, phase problem					no boule
25	B32-413	Y_2SiO_5	6% Tm	good crystal, no fluorescence	---	1.5	10	0.3	
26	B23-112	Y_2SiO_5	30% Er	good crystal, cracked on cooling	---	1	10	0.3	Sent 10/92
27	B23-113	$CaLa_4(SiO_4)_3O$	6% Tm	bubble core, blue fluorescence	20° off (00.1)	1	10	0.3	
28	B23-114	$CaLa_4(SiO_4)_3O$	30% Er	many bubbles, cracked badly	20° off (00.1)	1	5	0.3	Sent 10/92
29	B24-87	$CaY_4(SiO_4)_3O$	6% Tm	smoke which anneals out, uncracked	10° off (00.1)	1	10	0.3	line14,36 boule to M Seltzer,11/93
30	B24-88	$CaLa_4(SiO_4)_3O$	0.1% Cr 30% Er	purple, cracked, many scatter sites	10° off (00.1)	1	5	0.3	

Table IV

List of Grown Oxides

Serial #	Run #	Host	Dopant at %	Comments	Growth Axis	Pull Rate mm/h	Rot. Rate RPM	% O_2	
31	B23-116	Y_2SiO_5	0.1% Cr	dichroic (blue-clear), cracked, no scatter		1	8	0.3	
32	B23-117	Y_2SiO_5	0.1% Cr 6% Tm	dichroic (blue-tan), uncracked, no scatter		1	5	0.35	
33	B24-89	$CaLa_4(SiO_4)_3O$	0.1% Cr 30% Er	Cracked, use for seeds	near (00.1)	1	5	0.3	
34	B23-118	$CaLa_4(SiO_4)_3O$	0.1% Cr 2% Tm	Many scattering sites	30° off (00.1)	1	5	0.3	
35	B23-119	$CaLa_4(SiO_4)_3O$	0.1% Cr 0.2% Ho	Cracked, scatter in top only	20° off (00.1)	1	5	0.3	
36	B23-120	$CaLa_4(SiO_4)_3O$	0.1% Cr 0.4% Ho	No cracks, no scatter	(00.1)	1	5	0.3	
37	B24-90	Y_2SiO_5	0.1% Cr 2% Tm	dichroic (blue-tan), uncracked, no scatter		1	5	0.3	
38	B24-91	$Ca_3ZrNbGa_3O_{12}$	Nd	no boule, crucible leaked					no boule
39	B24-92	$Bi_4(SiO_4)_3$	---	no boule, glass forming melt					no boule
40	B24-93	$Bi_4(GeO_4)_3$	---	seed boule, colorless		3	5	air	no boule
41	B24-94	$Bi_4(GeO_4)_3$	0.1% Cr	yellow green, no red fluorescence		1.5	10	air	
42	B24-95	$Bi_4(GeO_4)_3$	0.1% Cr 2% Tm	rough interface, full of scatter		1.5	10	air	

Table IV

List of Grown Oxides

Serial #	Run #	Host	Dopant at %	Comments	Growth Axis	Pull Rate mm/h	Rot. Rate RPM	% O_2	
43	B23-122	YVO_4	10%Er	uncracked, green fluorescence	(001)	1.5	5	0.86	Sent 10/92
44	B32-431	YVO_4	6%Tm	gold color, largely uncracked	(001)	1.5	5	0.86	
45	B36-332	Y_2SiO_5	5%Yb	colorless, large crack, bubble core	---	1.5	5	0.3	
46	B32-434	YVO_4	12%Tm	gold color, largely uncracked	(001)	1.5	5	0.82	
47	B36-333	GSAG	5%Yb	colorless, cracks in top, high strain	(111)	1.5	5	.3	
48	B23-124	SGGM	2%Nd	90mm long, smoke, lineage // c axis, some Ir scatter	(100)	1	5	3.0	
49	B36-334	GSGG	20%Er	yellow fluor., 8mm flat interface at end	(111)	1.5	30	1.0	Sent 10/92
50	B36-335	GSGG	40%Er	weak yellow fluor., 25mm flat interface at end	(111)	1.5	30	1.0	Sent 10/92
51	B36-336	GGG	20%Er	weak yellow fluor.	(111)	1.5	35	2	Sent 10/92
52	B36-337	GGG	30%Er	no fluor.	(111)	1.5	35	2	Sent 10/92
53	B36-338	GGG	40%Er	no fluor.	(111)	1.5	35	2	Sent 10/92
54	B36-339	YSGG	5%Yb	colorless, cracked in top, no scatter	(100)	1.5	42	1.5	
55	B23-127	Y_2SiO_5	2%Tm	cracked after growth, blue fluor.	---	1.5	10	0.3	

Table V
Neodymium Doped Crystals

Host	Nd Concentration	Comments	Published
$SrGdGa_3O_7$ SGGM	2% , 4%	8nm FWHM @ 809nm, 212μs lifetime with 4%Nd, σ_{SE} = $6.6x10^{-20}$ cm^2, lased with 40% slope efficiency	x
$La_3Ga_5SiO_{14}$ LGS	2% , 4%	5nm FWHM @ 809nm, 195μs lifetime with 4%Nd, σ_{SE} = $7.4x10^{-20}$ cm^2, lased with 48% slope efficiency	x
$La_3Ga_5GeO_{14}$ LGG	2%	7nm FWHM @ 809nm, 220μs lifetime, σ_{SE} = $8x10^{-20}$ cm^2, difficult to grow	x
YVO_4	1.2% , 1.6%	spectroscopic samples fabricated	
$LuLiF_4$	2%	spectroscopy identical to $YLiF_4$	

Table VI
Thulium Doped Crystals

Host	Tm Concentration	Comments	Published
$SrGdGa_3O_7$ SGGM	3% , 6%, 12%	15nm FWHM @ 790nm, 6900μs lifetime with 12% Tm, σ_{SE} = 0.63×10^{-20} cm^2	x
Y_2SiO_5 YOS or YSO	2% , 6%	2.1nm FWHM at 791nm	x
$CaLa_4(SiO_4)_3O$ CaLaSOAP	6%	5nm FWHM at 791nm for E//c	x
$CaY_4(SiO_4)_3O$ CaYSOAP	6%	5nm FWHM at 790nm for E//c, abs. coeff. ~$34cm^{-1}$ (or 6 times Tm:YAG), lifetime 585μs, σ_{SE} = 1×10^{-20} cm^2, lased CW at 1.94μm with 32% slope efficiency, crystal length 0.57mm	x
YVO_4	6% , 12%	spectroscopic sample fabricated	

strong absorption permits better mode matching to the diode pump laser. A crystal 0.57 mm thick lased CW at 1.94 μm which is a wavelength of interest for medical applications. The fluorescent lifetime was 585 μs and the stimulated emission cross section $1x10^{-20}$ cm^2.

A lot of time has been devoted to the Er^{3+} doped crystals which can lase in the vicinity of 2.9 μm. It is interesting that high doping levels of 10-40% can be used without any significant quenching of the lifetime. The crystals grown under our program are listed in Table VII. So far only one of these has been tested extensively. More will be examined in the future.

The Yb^{3+} can be diode pumped near 0.9 μm with high efficiency and lased at 1.04 μm. While we did not dwell on this system for the purpose of optimization, we did prepare a few crystals for examination. These are listed in Table VIII. Samples were fabricated for spectroscopic evaluation. Several groups at Livermore, CREOL, and other places have examined Yb^{3+} thoroughly.

Systems which are doped with chromium and a rare earth are particularly valuable. We have examined a number of crystal hosts where there are exclusively tetrahedral sites likely to incorporate Cr^{4+}. This ion has wide absorption bands and can be pumped near 532, 600-900, and even at 1064 μm. Fluorescence can occur over a range of 1050-1600 nm for the single ion, leading to a possible tunable laser. However, with the proper rare earth, an efficient energy transfer may occur. In Table IX we have listed a number of double doped crystals involving Tm, Ho, or Er as the rare earth. The complex anions are all tetrahedrally coordinated to favor the inclusion of Cr^{4+}. At the time

Table VII
Erbium Doped Crystals

Host	Er Concentration	Comments	Published
Y_2SiO_5 YOS or YSO	30%	spectroscopic sample fabricated	
$CaLa_4(SiO_4)_3O$ CaLaSOAP	30%	10nm FWHM at 980nm, 3mm monolithic laser rod fabricated for diode end-pumping at 980nm	
YVO_4	10%	spectroscopic sample fabricated	
$Gd_3Ga_5O_{12}$ GGG	20, 30, 40%	spectroscopic samples fabricated	
$Gd_{2.96}Sc_{1.9}Ga_{3.14}O_{12}$ GSGG	20, 40%	spectroscopic samples fabricated	x

Table VIII
Ytterbium Doped Crystals

Host	Yb Concentration	Comments
Y_2SiO_5 YOS or YSO	5%	spectroscopic sample fabricated
$Y_3Sc_2Ga_3O_{12}$ YSGG	5%	spectroscopic samples fabricated
$Gd_3Sc_2Al_3O_{12}$ GSAG	5%	spectroscopic samples fabricated

Table IX
Chromium - Rare Earth Doped Crystals

Host	Cr^{4+} & RE Concentration	Comments
Y_2SiO_5	0.1% Cr	spectroscopic sample fabricated
Y_2SiO_5	0.1% Cr, 2% Tm	spectroscopic sample fabricated
Y_2SiO_5	0.1% Cr, 6% Tm	spectroscopic sample fabricated
$CaLa_4(SiO_4)_3O$	0.1% Cr, 2% Tm	spectroscopic sample fabricated
$CaLa_4(SiO_4)_3O$	0.1% Cr, 6% Tm	2μm fluorescence observed when pumped into Cr^{4+} bands
$CaLa_4(SiO_4)_3O$	0.1% Cr, 0.2% Ho	spectroscopic sample fabricated
$CaLa_4(SiO_4)_3O$	0.1% Cr, 0.4% Ho	spectroscopic sample fabricated
$CaLa_4(SiO_4)_3O$	0.1% Cr, 30% Er	spectroscopic sample fabricated
$Bi_4(GeO_4)_3$ BGO	0.1% Cr	spectroscopic sample fabricated
$Bi_4(GeO_4)_3$	0.1% Cr,.2%Tm	spectroscopic sample fabricated

of this writing only a few samples were examined for their spectroscopy. By way of illustration we show in Fig. 9 two of the grown crystals. A brief check of CaLaSOAP doped with Cr^{4+} and Tm^{3+} showed that pumping into the broad Cr^{4+} absorption bands result in 2 micron Tm fluorescence, which confirms energy transfer. The broad absorption relaxes the wavelength control requirement for the pump diode and may lead to a very simple diode pumped rare earth laser.

3.4 Fluoride Hosts for Nd

A large number of fluorides have been investigated since the first work with Nd:CaF_2[22]. The host materials can be classed as either those with an ordered structure (i.e. $LiFY_4$) or those with a disordered structure where more than one lattice site may be occupied by the active ion. Table X lists some of the better known fluoride lasers.

Nd:$LiYF_4$ is a good material for diode pumping, because it has the features of long lifetime, large cross-section, fairly broad absorption at the exciting wavelength, and high optical quality. This material has already been commercialized and though there are still some quality problems, it required no attention here. There are other crystals of good potential which have not been extensively examined. One of the chief reasons is that growth difficulties have prevented them from being actively pursued in a serious way.

One important property of many fluorides is that they do not possess the cubic structure and, therefore, are not isotropic in their physical properties. This has advantages for some applications where, for instance, polarized output may be desirable.

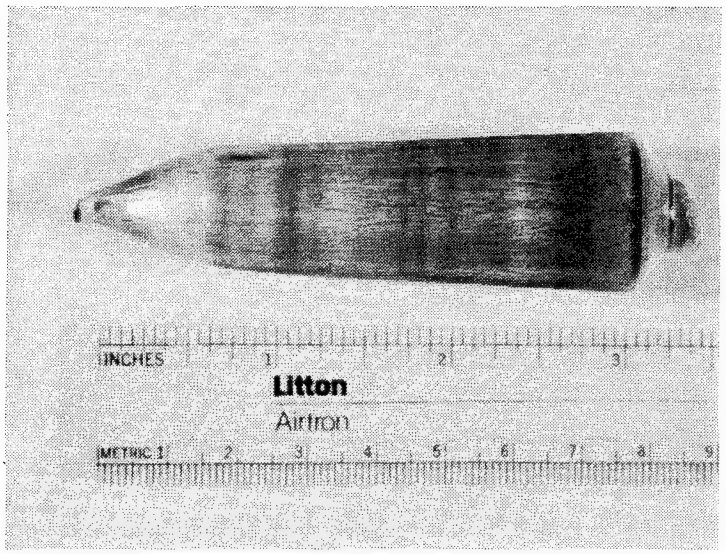

Figure 9 Typical Crystals Grown. Top: 0.1%Cr, 6%Tm:Y_2SiO_5
Bottom: 0.1%Cr, 0.4%Ho: CaLaSOAP

Table X

Examples of the Better Known Fluoride Lasers

Host	Crystal Structure	Active Ion	Wavelength (μm)	Lifetime (ms)
$LiYF_4$	Tetragonal	Nd	1.053	.05
$NaYF_4$	Hexagonal	Nd	1.04-1.07	0.3
LaF_3	Hexagonal	Nd	1.063	0.7
$Na_5Y_9F_{32}$	Orthorhombic	Nd	1.307	1
$NaYF_4$	Hexagonal	Ho	1.94-2.1	12
$BaYb_2F_8$	Monoclinic	Er	1.96	-
$BaEr_2F_8$	Monoclinic	(Tm)Ho	2.063	-
BaY_2F_8	Monoclinic	(Er,Tm)Ho	2.17	16
$Ba(Y,Er)_2F_8$	Monoclinic	Dy	3.02	7

As a starting point representative Nd-doped materials from various fluoride compositions were grown and additional growth runs were performed on those which seemed to be most promising. Spectroscopic samples from the initial series sufficed. Table XI lists other new hosts for the entire 1-5 micron range.

It was virtually impossible to consider every crystal of interest. Thus, only those suggested as good candidates by past work were examined. As a start, we began with crystals grown from the group (Na,K) (Y,La) F_4. $NaYF_4$ has been shown to be a good candidate by virtue of long lifetime and broad absorption resulting from two-site occupancy of Nd[23]. The K homologue should behave similarly due to similar ratios of Na/Y and KY.

The crystal structure [24] of $NaYF_4$ is hexagonal with a=5.967A and c=3.523A. The structure contains two distinct rare earth sites, both of which are surrounded by nine fluorine ions in the shape of a trigonal prism. This dual site occupancy probably is the reason for broadened absorption and emission lines. The emission cross section and fluorescent lifetime are both larger than Nd:YAG or Nd:YLF. This makes the host quite interesting for all rare earth doping. Furthermore the host is transparent out to about 11μm. A schematic of the structure is given in Fig. 10.

The phase diagram [25] of the system NaF-YF_3 is reproduced in Fig. 11. It is very unfortunate that $NaYF_4$ is incongruently melting since this prevents easy crystal growth of sizable pieces of material. The shaded area of Fig. 11 indicates where the $NaYF_4$ solid phase is stable along with some liquid. There

Table XI

Potential Fluoride Hosts for 1-5 μm Lasers

Host	Crystal Structure	Comments
$LiLuF_4$	Tetragonal	Congruent melting, uniform doping
KLn_3F_{10}	Cubic	Congruent, good host for all LN
$LiCaAlF_6$	Hexagonal	Good host for Nd, disorder
Li_3GdF_6	Hexagonal	Good Nd potential, not examined
$CaGeF_6$	Cubic	Possible two site occupancy
$CaZnF_4$	Cubic-hexagonal	Possible two site occupancy
Cs_2KLaF_6	Cubic	Very low Nd concentration quenching
$BaMgF_4$	Tetragonal	Linewidth broadening
Ba_2MgAlF_9	Cubic	Disorder
$LiBaAlF_6$	Cubic	Two site occupancy
$Na(Ce,La)F_4$	Hexagonal	Good host for small Ln, disorder
$NaLu_2F_7$	Hexagonal	Good host for large Ln, not examined
$K(Y,La)F_4$	Hexagonal	Good host for Nd, not examined
$Li_3Na_3Ga_2F_{12}$	Cubic	Garnet structure
$KMgF_3$	Cubic	Potential for tunability

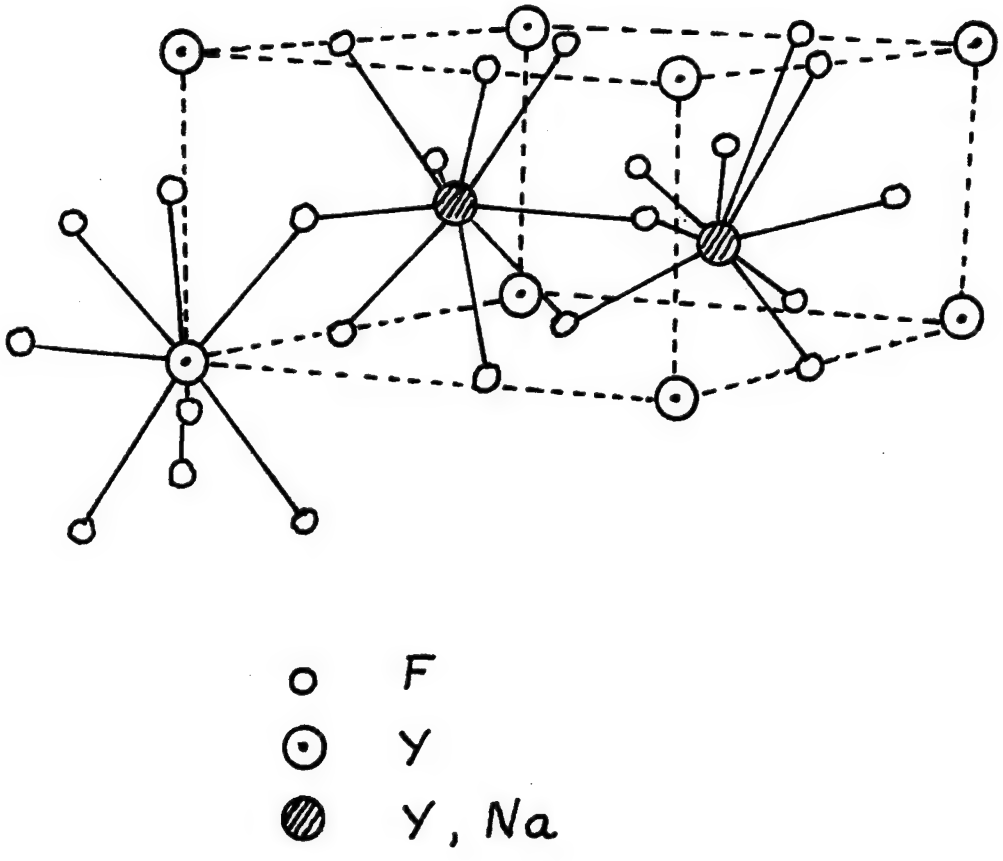

Fig. 10 Structure of $NaYF_4$

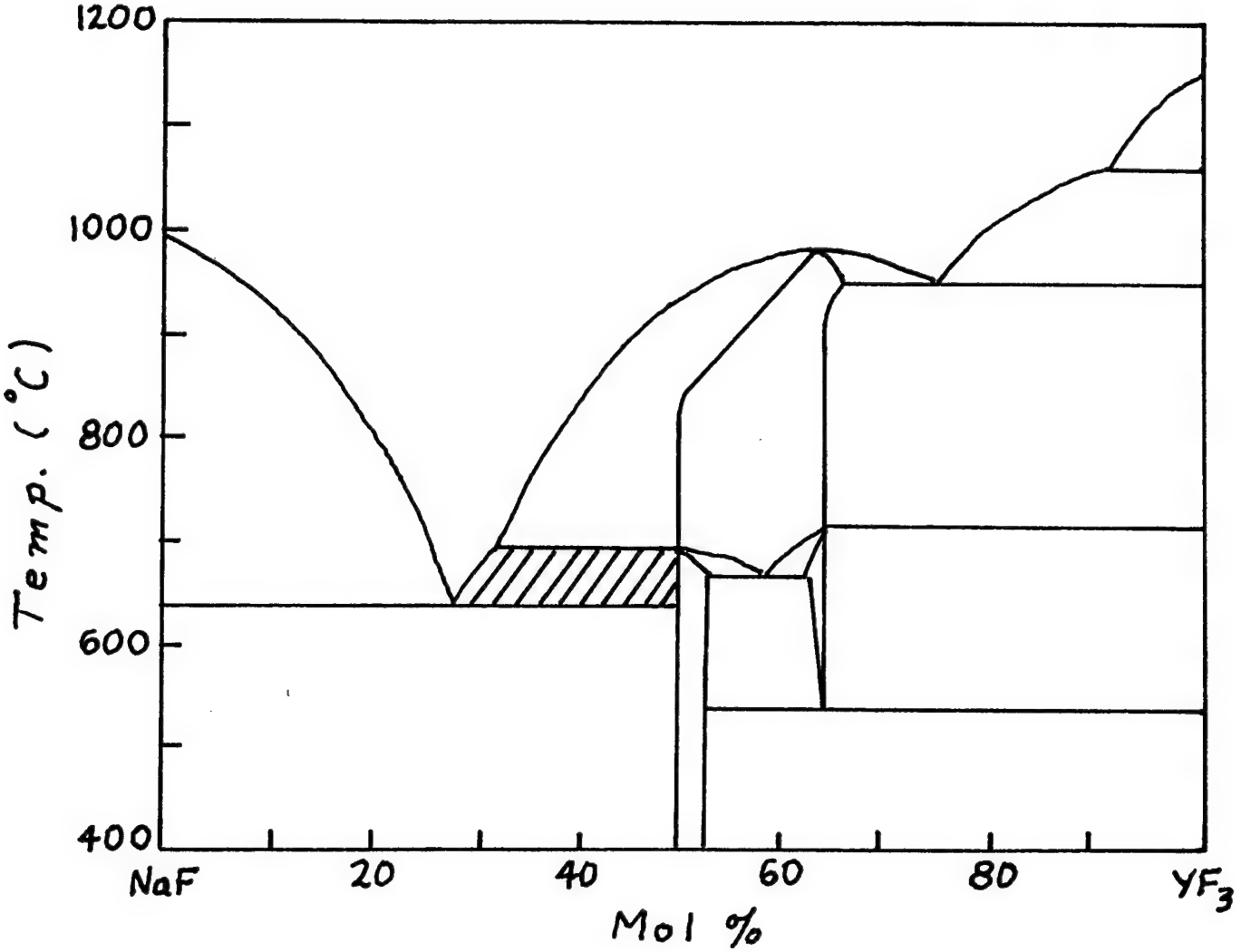

Fig. 11 Phase Diagram of $NaF-YF_3$ System

the crystal can be grown from a solution by a modified Czochralski method. This is generally performed by preparing a composition of 30-32 mole % YF_3, slow cooling the melt, and attaining seeded solution growth. One is faced with two other difficulties. The temperature range of crystallization is small, i.e. 20-40^0, so that excellent thermal control is required. The phase diagram is for pure $NaYF_4$ and any dopants will modify it somewhat. Thus low concentrations of dopants such as Er, Tm, or Ho with a size about equal to Y will be easier to grow than Nd, Pr or other dopants with a large size.

All of our crystal growth attempts at Airtron were devoted to Er:$NaYF_4$. The Er offered several transitions in the infrared and was not investigated previously. Melts of pure NaF-YF_3 at 31 mole % YF_3 were prepared and seed crystals were nucleated by several methods. A cooled platinum wire was inserted, the melt was slow cooled, and small crystals were placed in contact with the melt surface. All of these did not result in larger high quality seeds. Generally the obtained material was cloudy and polycrystalline. A cloudy melt sometime indicates possible contamination with O_2; however all of our growth was conducted in an HF atmosphere. Several further trials were attempted with Er doping levels in the range of 10-25%. No good single crystals were obtained and most of the runs yielded pieces of only 1-2 mm. These were sufficient for some spectroscopic characterization but not for any laser testing. The length of time devoted to $NaYF_4$ growth with a poor yield of single crystal dictated that this system was not amenable to further development. Therefore Airtron ceased work on this crystal.

Some attention was given to the $LiSrAlF_6$ structure as a possible host for the smaller size rare earths. The largest ion in the crystal is the Sr^{2+}. This ion is also larger than Ho^{3+}, Er^{3+}, or Tm^{3+} even though the charge is different and some compensation may be required. Two runs were made with up to 10% Tm doping. The Na^{1+} ion was coupled with the Tm^{3+} to attempt substitution at two Sr^{2+} sites. These runs led to the production of polycrystalline material and indicated that the phase equilibria are complicated. It should be noted that the Sr^{2+} is large enough to possible incorporate a U^{3+} ion. Two attempts were made on 1% U^{3+}:$LiSrAlF_6$ growth. The second trial yielded a small single crystal but with little U^{3+} incorporated. Undoubtedly the distribution coefficient is very small for some reason. While spectral data could be obtained, there was no indication of lasing action at these low U^{3+} levels.

The early success of lasing U^{3+} in CaF_2 prompted us to consider other mixed fluoride hosts which might incorporate a substantial amount of U^{3+}. Furthermore the U^{3+} has excellent potential for generating laser lines around 2.2-2.6 μm, some degree of tunability may be possible, and operation may occur at room temperature. Past work on these materials indicated two major problems; first the valence control of U^{3+} since it is easily oxidized to U^{4+} or U^{6+} and second the lack of suitable laser hosts. We believed both of these problems could be circumvented.

As explained in Section 2.2, the preparation of a purified product of UF_3 was invaluable. This was done by Al reduction of UF_4 prior to growth. This obviated the need for growth in H_2 or possible reduction of U^{4+} after growth by

radiation or chemical treatments. Both of the latter increase the brittle behavior of many fluorides. The choice of a host was dictated by its ability to incorporate U^{3+} and our general experience in growing large single crystals. The most useful host was $YLiF_4$. Since U^{3+} is only slightly larger than Nd^{3+}, we thought this represented our best opportunity for success.

The first boules of U^{3+}:$YLiF_4$ were attempted to be grown at a 1% doping level. Crystal growth was good along the {100} or a-axis configuration. The slight change in color along the boule indicated that the distribution coefficient was low and less than one as expected. An actual chemical analysis gave a value of about 0.13 for k. This is about 1/5 that for Nd^{3+} in $YLiF_4$ and reflects the larger size of U^{3+}. Thus some difficulty might be experienced in crystal growth or quality at the 1% U^{3+} level in the boule since about 7-8% U^{3+} has to be in the melt. One run was made with a 6% melt and a boule piece was obtained for spectroscopy.

Fig. 12 shows one of our best boules of U^{3+}:$YLiF_4$. It appears that this system is very worthy for continued research. The presence of only the U^{3+} in the crystal is indicated from spectroscopic data. At the low levels of U^{3+} in the crystal, no lasing was observed. Unfortunately further work on this material was curtailed. A summary of our fluoride growth runs is given in Table XII.

3.5 Crystal Fabrication and Deliveries

From all of the oxide growth runs of Table IV and the fluoride growth runs of Table XII, crystals were fabricated except for those cases where there was no yield. The latter included failed attempts, lack of size, polycrystalline material, or

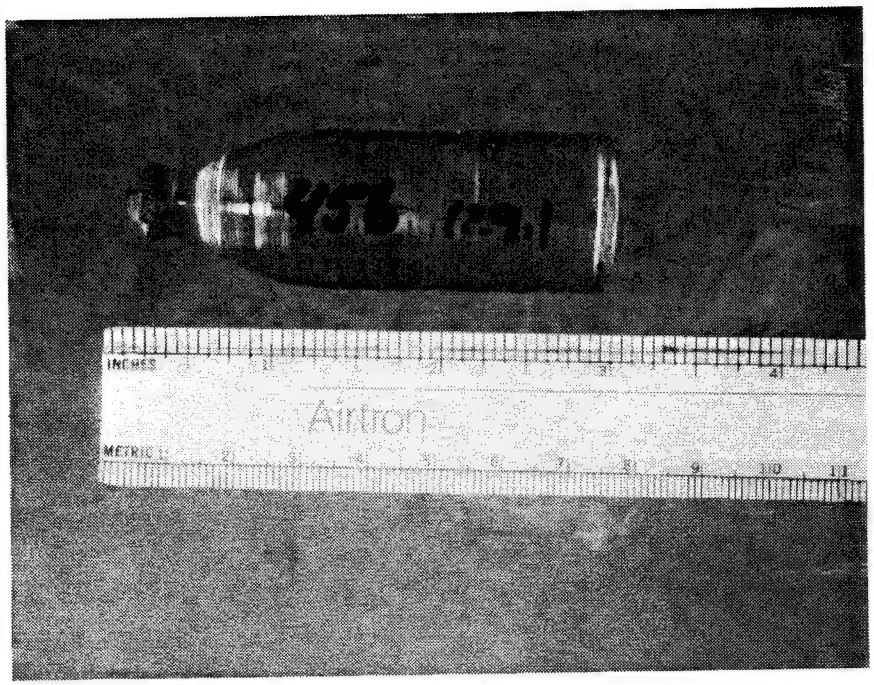

Fig. 12 Grown Boule of U^{3+}:$YLiF_4$

Table XII
List of Grown Fluorides

Serial #	Run #	Host	Dopant at %	Comments	Growth Axis	Pull Rate mm/h	Rot. Rate RPM	Atmos-phere	Final Boule Disposition
1	401	$NaYF_4$	---	seed run					
2	416	$LiSrAlF_6$	10% Tm	polycrystalline					
3	418	$LiSrAlF_6$	Tm+Na	attempt at chage compensation did not work, polycrystalline					
4	430	$LiYF_4$	1% U	small boule for spectroscopy	(100)	0.5	20	Ar	
5	431	$LiYF_4$	1% U	small boule for spectroscopy	(100)	0.5	20	Ar	
6	437	$LiLuF_4$	2% Nd	small boule for spectroscopy	(100)	0.5	20	Ar&HF	
7	443	$LiSrAlF_6$	1% U	furnace failed					
8	445	$LiSrAlF_6$	1% U	small crystal but very little U in crystal					
9	456	$LiYF_4$	1% U	small boule for spectroscopy	(100)	0.5	35	Ar&HF	
10	462	$LiYF_4$	6% U	small boule for spectroscopy	(100)	0.5	35	Ar&HF	

sometimes an equipment problem. Nearly 70-80% of all growth runs provided material for fabrication in a clear single crystal form. These crystals were usually 0.8-1.5 inches in diameter and 2-4 inches long. Thus adequate material was available for several fabricated pieces if necessary. All fabrication was performed in accordance with the final test objectives. Thus some crystals may have been rough cut in shapes of disks, cubes, or parallelepipeds where one, two, or three pairs of opposing faces were polished to transparency. These usually sufficed for preliminary spectroscopic investigations. For a more sophisticated active laser test, a full specification on the material was prepared such as dimensions, passive tests, and coatings. The material was then introduced as part of the Airtron laser crystal production schedule where all normal precautions were observed. Finished pieces were delivered normally to the Naval Research Laboratory for active testing. However some samples were provided to other test facilities within the Navy.

3.6 Test Results and Publications

All of the test data have been accumulated and presented at a variety of laser conferences in the form of oral presentations or published papers. We will not reproduce all of these in this report but a comprehensive list is given in Table XIII . The interested reader may consult these for further results on the given materials.

4.0 Conclusions

Under our growth program it has been possible to identify and prepare materials which can lead to efficient laser diode pumped systems. This was

Table XIII
List of Presentations and Publications

Conference Presentations

G.J. Quarles, L. Esterowitz, G.H. Rosenblatt, M.H. Randles, "Crystal Growth and Spectroscopic Characterization of Nd-Doped $SrGdGa_3O_7$," OSA Annual Meeting, paper ThJ2, Nov. 1991.

G.J. Quarles, L. Esterowitz, G.H. Rosenblatt, M.H. Randles, J.E. Creamer and R.F. Belt, "Characterization of Growth, Spectroscopy and Laser Properties of Rare-Earth-Doped Disordered Oxides," OE/LASE 93, SPIE Proceedings 1863, Jan. 1993.

G.H. Rosenblatt, G.J. Quarles, L. Esterowitz, M.H. Randles, J.E. Creamer and R.F. Belt, "Crystal Growth and Spectroscopic Characterization of Tm-doped Oxyapatites and Orthosilicates," in *Advanced Solid-State Lasers and Compact Blue-Green Lasers Technical Digest, 1993* (Optical Society of America, Washington, DC 1993), Vol. 2, pp. 147-149.

Publications

M.H. Randles, J.E. Creamer, R.F. Belt, G.J. Quarles and L. Esterowitz, "Disordered Oxide Crystals as Hosts for Diode-Pumped Lasers," OSA Proceedings on Advanced Solid-State Lasers 1992, Lloyd L. Chase and Albert A. Pinto, eds. (Optical Society of America, Washington, DC 1992), Vol. 13, pp. 318-321.

G.J. Quarles, L. Esterowitz, G.H. Rosenblatt, R. Uhrin and R.F. Belt, "Crystal Growth and Spectroscopic Properties of U^{3+} : $LiYF_4$," OSA Proceedings on Advanced Solid-State Lasers 1992, Lloyd L. Chase and Albert A. Pinto, eds. (Optical Society of America, Washington, DC 1992), Vol. 13, pp. 306-309.

M.H. Randles, J.E. Creamer, R.F. Belt, "Disordered Oxide Crystal Hosts for Diode Pumped Lasers," J. Crystal Growth *128* (1993) 1016-1020.

G.H. Rosenblatt, G.J. Quarles, L. Esterowitz, M. Randles, J. Creamer and R. Belt, "Crystal Growth and Spectroscopic Characterization of Tm-doped Oxyapatites and Orthosilicates," OSA Proceedings on Advanced Solid-State Lasers 1993, Albert A. Pinto and Tso Yee Fan, eds. (Optical Society of America, Washington, DC 1993), Vol.15, pp. 185-187.

G.H. Rosenblatt, G.J. Quarles, L. Esterowitz, M. Randles, J. Creamer and R. Belt, "Continuous Wave 1.94 μm $Tm:CaY_4(SiO_4)_3O$ Laser," submitted to Optics Letters (1993).

done by concentrating on host crystals with a disordered structure, multi-site occupation, or other artifact whereby the absorption and emission of the dopant is broadened slightly. Nearly 65 growth runs were achieved on about 20 different hosts doped with Nd, Ho, Er,Tm, U or their combinations. These were most useful for possible lasing operation through the 1-4 μm region. The majority of our materials were complex oxides with nearly 55 growth runs performed. Among the promising hosts were $SrGdGa_3O_7$, $La_3Ga_5SiO_{14}$, Y_2SiO_5, La_3GaGeO_{14}, $CaLa_4(SiO_4)_3O$, $CaY_4(SiO_4)_3O$, a variety of garnets, and YVO_4. Several fluorides such as $NaYF_4$, $LiSrAlF_6$, and $YLiF_4$ were also of interest particularly when doped with U^{3+}. The evaluation of these materials was achieved by preparation of standard samples for preliminary passive tests such as optical absorption, fluorescent emission lifetime, dopant levels, or other measurements. The most promising candidates were fabricated into suitable shapes such as rods, cubes, disks, or other configurations. Laser specifications were achieved and coatings applied for further active testing. About 40 samples were delivered on our program. Most crystals were tested actively at the Naval Research Laboratory or another Navy laboratory. The results of these investigations were presented in journals, or summarized in semi-annual reviews.

5.0 References

1. A complete issue is devoted to semiconductor lasers in IEEE J. Quantum Electronics, 25, No. 6, June 1989

2. R. Scheps, Appl. Optics 28, 89 (1989)

3. G.T. Forest, Laser Focus 24, p. 59 August, 1988

4. T.H. Allik et al. Optics Letters 14, 116 (1989)

5. J.L. Emmett, W.F. Krupke and J.B. Trenholme, Vol. IV, Physics of Laser Fusion, UCRL-53344, November, 1982, p.37

6. N.P. Barnes, M.E. Storm, P.L. Cross, and M.W. Skolant, Jr. Appl. Optics, to be published

7. A.A. Kaminskii, Laser Crystals, Springer-Verlag, New York, 1981 English Translation. The new Russian edition of 1989 has not been translated yet

8. S.R. Chinn, H.Y-P Hong, and J.W. Pierce, Laser Focus, p.64, May, 1976

9. H.Y-P Hong and S.R. Chinn, Mat. Res. Bull 11, 461 (1976)

10. G. Huber et al. IEEE J. Quantum Electronics 24, 920 (1988)

11. G.J. Kintz, R. Allen, and L. Esterowitz, Appl. Phys. Letters 50, 1553 (1987)

12. F. Anzel, S. Hubert, and D. Meichenin, Appl. Phys. Letters 54, 681 (1989)

13. M.E. Storm, and W.W. Rohrbach, Appl. Optics 28, 4965 (1989)

14. The coating calculation software was FILM STAR and written by Dr. Fred Goldstein

15. L. Esterowitz, R.C. Eckardt, and R.E. Allen, Appl. Phys. Lett., 35, 236 (1979)

16. Handbook of Laser Science and Technology-Volume I, ed. Martin J. Weber, CRC Press, Boca Raton, Florida (1982)

17. R.C. Stoneman, and L. Esterowitz, in Tunable Solid State Lasers, Vol. 5 of the OSA Proceeding Series, M.L. Shand and H.P. Jenssen, eds. (Optical Society of America, Washington, DC, 1989)pp. 157-160

18. R.C. Stoneman, private communication

19. L.D. Schearer, M. Leduc, D. Vivien, A-M Lejus, and J. Thery, IEEE J. Quant. Electronics, QE-22, 713-717 (1986)

20. A.P. Shkadarevich, in Tunable Solid State Lasers, Vol. 5 of the OSA Proceeding Series, M.L. Shand, and H.P. Jenssen, eds. (Optical Society of America, Washington, DC, 1989) pp.60-65

21. L.R. Black, D.M. Andrauskas, G.F. de le Fuente, and H.R. Verdun, Growth Characterization, and Application of Laser Host and Nonlinear Crystals, J.T. Lin, editor, Proc. SPIE 1104, 175-186 (1989)

22. L.F. Johnson, J. Appl. Phys. 33, 756 (1962)

23. D. Knowles, A. Cassanho, and H.P. Jenssen, Tunable Solid State Lasers, Vol. 5, of the OSA Proceeding Series, M.L. Shand, and H.P. Jenssen, eds. (Optical Society of America, Washington, DC, 1989) pp. 139-145

24. J.H. Burns, Inorg. Chem. 4, 881 (1965)

25. R.E. Thoma, G.M. Hebert, H. Insley, and C.F. Weaver, Inorg. Chem. 2, 1007 (1963)